Chromatin Loop Formation Induced by a Subtelomeric Protosilencer Represses *EPA* Genes in *Candida glabrata*

Eunice López-Fuentes,* Grecia Hernández-Hernández,* Leonardo Castanedo,* Guadalupe Gutiérrez-Escobedo,* Katarzyna Oktaba,† Alejandro De las Peñas,* and Irene Castaño*,[1]

*IPICYT, Instituto Potosino de Investigación Científica y Tecnológica, División de Biología Molecular, San Luis Potosí, SLP 78216, Mexico and †Departamento Ingeniería Genética, Centro de Investigación y de Estudios Avanzados del IPN (Cinvestav-Unidad Irapuato), C.P. 36824 Irapuato, Gto, México

ORCID IDs: 0000-0001-6794-5883 (E.L.-F.); 0000-0001-7204-5142 (G.G.-E.); 0000-0002-3950-5626 (K.O.); 0000-0002-2933-2856 (A.D.l.P.); 0000-0002-5968-2101 (I.C.)

ABSTRACT Adherence, an important virulence factor, is mediated by the *EPA* (Epithelial Adhesin) genes in the opportunistic pathogen *Candida glabrata*. Expression of adhesin-encoding genes requires tight regulation to respond to harsh environmental conditions within the host. The majority of *EPA* genes are localized in subtelomeric regions regulated by subtelomeric silencing, which depends mainly on Rap1 and the Sir proteins. *In vitro* adhesion to epithelial cells is primarily mediated by Epa1. *EPA1* forms a cluster with *EPA2* and *EPA3* in the right telomere of chromosome E (E_{-R}). This telomere contains a *cis*-acting regulatory element, the protosilencer Sil2126 between *EPA3* and the telomere. Interestingly, Sil2126 is only active in the context of its native telomere. Replacement of the intergenic regions between *EPA* genes in E_{-R} revealed that *cis*-acting elements between *EPA2* and *EPA3* are required for Sil2126 activity when placed 32 kb away from the telomere (Sil@-32kb). Sil2126 contains several putative binding sites for Rap1 and Abf1, and its activity depends on these proteins. Indeed, Sil2126 binds Rap1 and Abf1 at its native position and also when inserted at −32 kb, a silencing-free environment in the parental strain. In addition, we found that Sil@-32kb and Sil2126 at its native position can physically interact with the intergenic regions between *EPA1-EPA2* and *EPA2-EPA3* respectively, by chromosome conformation capture assays. We speculate that Rap1 and Abf1 bound to Sil2126 can recruit the Silent Information Regulator complex, and together mediate silencing in this region, probably through the formation of a chromatin loop.

KEYWORDS *Candida glabrata*; *cis*-elements; transcriptional regulation; protosilencer; *EPA* genes; Rap1; chromatin loop

REGULATION of transcription, DNA replication, recombination, and DNA damage repair in eukaryotes depends critically on the chromatin structure. The nucleus is organized in different subcompartments in which the chromosomes are nonrandomly positioned, adopting *ad hoc* conformations for each process (Duan *et al.* 2010). Regulatory *cis*-acting DNA regions for gene expression distantly localized in chromosomes are thought to be brought into physical proximity with their gene targets through DNA loop formation. It is proposed that chromatin loops associate in space and lead to the organization of chromatin into functionally related topological domains (Bonev and Cavalli 2016). In addition, the telomeres, which are specialized structures at the ends of the chromosomes, are generally found in clusters around the nucleus at the nuclear periphery (Palladino *et al.* 1993) and excluded from the nucleolus (Therizols *et al.* 2010). The adjacent sequences, called subtelomeres, are also mostly found near the nuclear periphery (Gotta *et al.* 1996; Hediger *et al.* 2002). In the baker's yeast *Saccharomyces cerevisiae*, there are several proteins that interact with telomeres and subtelomeres, which are enriched at the nuclear periphery, such as the Silent Information Regulator (SIR) complex, (formed by the Sir2, Sir3, and Sir4 proteins) (Andrulis *et al.* 1998) and the repressor-activator protein 1, Rap1 (Gotta *et al.* 1996). The interaction of these proteins with the telomeres and subtelomeres leads to the formation of a repressive form of chromatin called heterochromatin.

doi: https://doi.org/10.1534/genetics.118.301202
Manuscript received May 31, 2018; accepted for publication July 9, 2018; published Early Online July 12, 2018.
Supplemental material available at Figshare: https://doi.org/10.25386/genetics.6405983.
[1]Corresponding author: División de Biología Molecular, Instituto Potosino de Investigación Científica y Tecnológica (IPICYT), Camino a la Presa San José 2055, Col. Lomas 4a, San Luis Potosí 78216, México. E-mail: icastano@ipicyt.edu.mx

Heterochromatin in *S. cerevisiae* is found at the ribosomal DNA (rDNA) tandem array, the silent mating loci, and the telomeres. Transcriptional silencing close to the telomeres is also called the telomere position effect and is found in many organisms in addition to *S. cerevisiae*, such as fission yeast (*Schizosaccharomyces pombe*), the fruit fly *Drosophila melanogaster*, the sleeping sickness parasite *Trypanosoma brucei*, the malaria parasite *Plasmodium falciparum*, plants, and humans (Gottschling *et al.* 1990; Levis *et al.* 1993; Nimmo *et al.* 1994; Horn and Cross 1995; Scherf *et al.* 1998; Baur *et al.* 2001).

Transcriptional silencing is propagated from the telomere to the centromere, spanning the subtelomeric regions. Genes naturally located in the subtelomeric region are repressed in a promoter-independent fashion, although silencing at subtelomeric regions varies from telomere to telomere in fungi such as *S. cerevisiae* (Pryde and Louis 1999) and in the opportunistic fungal pathogen *Candida glabrata* (Rosas-Hernández *et al.* 2008). Notoriously, in some pathogenic organisms, several genes encoding known or suspected virulence factors are localized at subtelomeric regions. For example, in the case of unicellular parasites, the *var* genes of *P. falciparum* (Gardner *et al.* 2002) and the single variant-specific surface glycoprotein gene (VSG) of *T. brucei* are located adjacent to a telomere (Horn and Cross 1995); and in the pathogenic fungus, *Pneumocystis carinii*, the major surface glycoprotein (MSG) gene family is located near chromosomes ends (Keely *et al.* 2005).

C. glabrata is a haploid budding yeast, which has emerged as an important nosocomial fungal pathogen associated with an attributable mortality of ∼30% (Klevay *et al.* 2009). It normally resides as a commensal in the flora of healthy human mucosal tissues, to which it adheres tightly, but can cause infections in immunocompromised patients (Pfaller and Diekema 2007).

In *C. glabrata*, most of the *EPA* (Epithelial Adhesin) genes encoding adhesins are located in subtelomeric regions. The Epa family is the largest family of cell wall proteins in *C. glabrata*, with at least 17 and up to 23 paralogs, depending on the strain. Epa1 mediates almost all the adherence to epithelial cells *in vitro* (Cormack *et al.* 1999), and Epa6 and Epa7 are also functional adhesins involved in kidney colonization (Castaño *et al.* 2005).

The variant gene families located in subtelomeric regions are not restricted to pathogenic species, for example *S. cerevisiae* contains four of the five members of the *FLO* gene family of cell wall proteins in subtelomeric regions (Guo *et al.* 2000). The expression of some subtelomeric genes in *S. cerevisiae* is regulated by transcriptional silencing (Ellahi *et al.* 2015), which requires different proteins, such as Rap1, which binds to telomeric repeats, yKu70, yKu80, the SIR complex, Rif1, and other proteins (Kyrion *et al.* 1993; Luo *et al.* 2002; Thurtle and Rine 2014; Gartenberg and Smith 2016). In addition, *cis*-acting elements called silencers and protosilencers aid in transcriptional silencing by binding sequence-specific factors that lead to the recruitment of the SIR complex. Silencers are negative regulatory elements composed of a combination of binding sites for various silencing factors (Fourel *et al.* 1999). At telomeres, the terminal repeated $TG_{1–3}$ sequences serve as silencers. Protosilencers may act in synergy with silencers or other protosilencers to stabilize and extend the propagation of heterochromatin (Fourel *et al.* 2002).

In *C. glabrata*, subtelomeric silencing requires the SIR complex, as well as the Rif1, Rap1, and the yKu proteins, and can extend > 20 kb toward the centromere (De Las Peñas *et al.* 2003; Domergue *et al.* 2005; Rosas-Hernández *et al.* 2008). Different telomeres in *C. glabrata* have different protein requirements for silencing. For instance, the proteins yKu70 and yKu80 are not required in the right telomere of chromosome E (E_{-R}) where *EPA1* forms a cluster with the *EPA2* and *EPA3* genes. This independence of yKu proteins is due to a *cis*-acting element, the protosilencer Sil2126, which has overlapping functions with the yKu proteins (Juárez-Reyes *et al.* 2012) (Figure 1A). The Sil2126 element can mediate silencing of the *URA3* reporter when both are inserted 32 kb away from the telomere in the right telomere of chromosome E, but not when they are placed at similar distances in other telomeres. Sil2126 contains a putative binding site for Rap1 and another for the ARS-binding factor (Abf1) in the 5′ fragment (Juárez-Reyes *et al.* 2012). In addition to Sil2126, we have identified another *cis*-acting element 300 bp downstream from *EPA1*, called the negative element (NE) (Figure 1A), which negatively regulates *EPA1* expression in a promoter-specific fashion (Gallegos-García *et al.* 2012).

In this work, we wanted to understand the mechanism by which Sil2126 extends gene silencing in the subtelomeric region of telomere E_{-R} and uncover elements in this region that are required for its telomere E_{-R}-specific activity. We show that the protosilencer Sil2126 recruits Rap1 and Abf1, both when it is located in its original position between *EPA3* and telomere E_{-R} and when moved 32 kb away from the telomere (Sil@-32kb), where there is normally no silencing. In addition, we observe that Sil@-32kb interacts with the *EPA1-EPA2* intergenic region by 3C assay (chromosome conformation capture). Furthermore, Sil2126 at its native locus strongly interacts with *cis*-acting elements between *EPA2* and *EPA3*. We propose that Sil2126 induces the formation of alternative chromatin loops mediated by protein–protein interactions between silencing proteins recruited to Sil2126 and these intergenic regions to extend the silencing.

Materials and Methods

Strains

All strains and plasmids used are listed in Supplemental Material, Tables S1 and S2, respectively.

Media

C. glabrata strains were grown at 30° in plates with YPD medium, which contained 10 g/liter of yeast extract and 20 g/liter of peptone, supplemented with 2% glucose and 2% agar. If necessary, culture plates were supplemented with

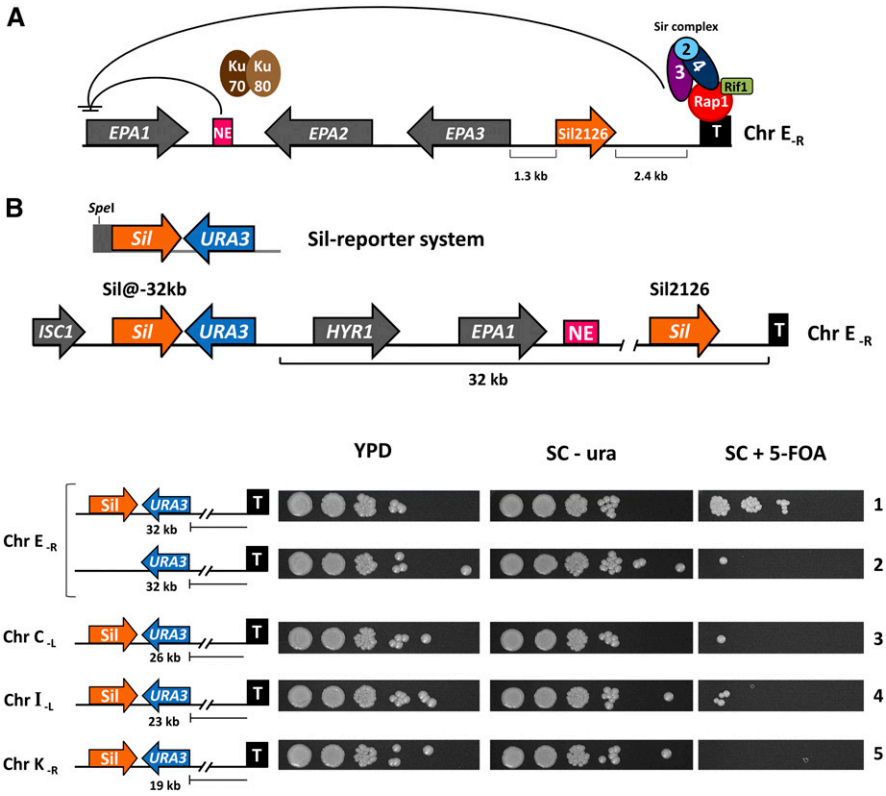

Figure 1 Sil2126 requires the context of telomere (T) E_{-R}. (A) Map of the T E_{-R} showing the relevant *cis*-acting elements and the proteins required for subtelomeric silencing. This region contains the *EPA1*, *EPA2*, and *EPA3* genes indicated by arrows. The protosilencer Sil2126 is drawn as an orange arrow between *EPA3* and the T. Rap1 (red circle) binds to the T repeats, and recruits the SIR complex (Sir2, Sir3, and Sir4) and Rif1 (green rectangle). A second *cis*-acting element called the negative element (NE, represented as a pink rectangle) represses *EPA1* expression in a promoter-dependent way and requires the yKu proteins (yKu70 and yKU80). Silencing can spread from the T, with the contribution of the protosilencer Sil2126, to up to > 20 kb to the *EPA1* gene. (B) Top: schematic representation of the Sil-reporter system consisting of a PCR product containing a 665-bp integration region (gray box), cloned immediately adjacent to the 5′ end of the Sil2126 element, followed by the *URA3* reporter gene with its own promoter. Middle: Sil2126 integrated between *ISC1* and *HYR1*, which is 32 kb from the right T of chromosome (Chr) E (E_{-R}, Sil@-32kb); the *Spe*I site used to linearize and integrate the vector, is indicated. Only the genes from *ISC1* to *EPA1* are shown. Note the discontinuity from the NE close to the 3′ UTR of *EPA1* up to the native Sil2126 element near the T. Bottom: the Sil-reporter system was integrated in different chromosomes at similar distances from the indicated T (shown to the left of each line). In Chr E_{-R}, the Sil-reporter system (line 1) and the negative control (*sil*-) consisting only of the *URA3* reporter (line 2) was integrated at −32 kb. The Sil-reporter system in Chr C_{-L} was integrated at −26 kb from the T (line 3); in Chr I_{-L}, at −23 kb (line 4); and in Chr K_{-R}, at −19 kb (line 5) from the T. The level of silencing of the *URA3* reporter was tested using a growth plate assay on SC –ura or SC + 5-FOA plates. The number of viable cells used for each experiment is estimated by the growth on rich YPD media. Strains were grown to stationary phase in YPD, after which 10-fold serial dilutions were made in sterile water and equal numbers of cells were spotted onto the indicated plates. Plates were incubated for 48 hr at 30° and photographed.

hygromycin (Invitrogen, Carlsbad, CA) 440 μg/ml or Nourseothricin 100 μg/ml (streptothricin sulfate, NTC, cloNAT, catalog number N-500-1). We used synthetic complete (SC) medium for the plate growth assays. This medium contains 1.7 g/liter yeast nutrient base [without $(NH_4)_2SO_4$ and amino acids] and 5 g/liter $(NH_4)_2SO_4$, and is supplemented with 0.6% casaminoacids and 2% glucose. To test the silencing level, 0.9 g/liter 5-FOA (Toronto Research Chemicals) and 25 mg/liter uracil were added to the SC medium. Minimal medium was used for the chromatin immunoprecipitation (ChIP) and 3C assays. This medium contains 1.7 g/liter yeast nutrient base and 5 g/liter $(NH_4)_2SO_4$, and is supplemented with 2% glucose and 25 mg/liter uracil.

Bacteria were grown at 30° in LB medium as described previously by Ausubel *et al.* (2001). LB medium contains 5 g/liter yeast extract, 10 g/liter tryptone, and 5 g/liter NaCl. If necessary, 1.5% agar was added. All plasmid constructs were introduced via electroporation into the DH10 strain. If needed, 50 mg/ml carbenicillin (Invitrogen) was added for plasmid selection.

Yeast transformation

Yeast transformation was performed using the lithium acetate protocol as described previously by Castano *et al.* (2003).

Plate growth assays

The level of silencing or expression of the *URA3* reporter was assessed using a plate growth assay as described previously (De Las Peñas *et al.* 2003; Castaño *et al.* 2005). Briefly, strains containing the different *URA3* insertions were grown at 30° in YPD for 48 hr to stationary phase. The cultures were adjusted to an OD_{600} of 1 with sterile water. Next, 10-fold serial dilutions were made in 96-well plates. A total of 5 μl of each dilution was spotted onto YPD, SC-Ura, and SC +5-FOA plates, and plates were incubated for 48 hr at 30° and photographed.

GFP expression by flow cytometry

Strains were grown for 48 hr at 30° in SC medium supplemented with uracil when it was necessary. Cultured cells were diluted into fresh media to induce *EPA1* expression and samples were taken every 2 hr. Activity of the *EPA1* promoter was measured by determining fluorescence of the GFP reporter by FACS analysis using a BD FACSCalibur flow cytometer with Cell Quest Pro software, and results were analyzed with FlowJo software.

Western blot assay

We constructed epitope-tagged versions of each protein tested. Rap1 and Sir3 were tagged with Flag epitope at the

C-terminus and integrated in their native loci, respectively. To test Abf1, we constructed a plasmid containing an N-terminal fusion of cMyc with Abf1 under the inducible promoter P_{MT1}. The strains were grown in YPD at 30° and harvested in stationary phase. The protein extraction and western blot assays were done as previously described with minor modifications (Orta-Zavalza *et al.* 2013; Robledo-Márquez *et al.* 2016). Briefly, cells were resuspended in lysis buffer [45 mM HEPES, 400 mM potassium acetate, 0.5% Nonidet P-40, 1 mM EDTA, 1 mM DTT, 1 mM PMSF, and 1× Complete protease inhibitor cocktail (Roche)], 100 μl of zirconia beads were added, and cells were broken using FastPrep-24 (MP Biomedicals) equipment, with three pulses for 60 sec at 6 m/sec. The cells were centrifuged at 15,000 rpm for 40 min at 4°, the supernatant was recovered, and the protein content was determined by Bradford assay. Next, 50 μg of total protein were mixed with 2× SDS loading buffer, preheated (95° for 8 min), and then loaded onto a 10% SDS-polyacrylamide gel. After electrophoresis, the proteins were blotted onto PVDF membranes (Bio-Rad, Hercules, CA) and probed overnight with anti-Flag (Sigma [Sigma Chemical], St. Louis, MO) at a final concentration of 3 μg/ml. After washing, the membrane was probed with a goat–mouse horseradish peroxidase-conjugated secondary antibody (Merck). The signal was detected by ECL chemiluminiscence reagents (Pierce Chemical, Rockford, IL) and recorded using a Bio-Rad ChemiDoc MP System equipped with chemiluminescence.

ChIP assay

Yeast cultures (150 ml) were grown in minimal medium to an OD_{600} of 1 at 30°. Cells were fixed with 1% formaldehyde for 15 min at 25°. Cross-linking was quenched by the addition of glycine to 125 mM and incubation for 5 min. The cells were harvested, washed twice with TBS buffer (20 mM Tris-HCl (pH 7.5) and 150 mM NaCl], and transferred to 1.5 ml centrifuge tubes; yeast pellets were frozen at −80°. The cells were lysed with 500 μl lysis buffer [10 mM EDTA (pH 8), 50 mM Tris-HCl (pH 8), 1% SDS, 1 mM PMSF, and protease inhibitor ULTRA Tablet Mini/10 ml EASYpack (Roche)] added just before use, 500 μl glass beads were added, and cells were disrupted by vortexing for 30 sec before being placed on ice for 1 min (repeated 10 times). The chromatin in the lysates was sheared by sonication with 30 cycles (effective sonication time: 3 min 45 sec) at 20% amplitude in an Episonic multi-functional bioprocessor Model Oasis 180. The DNA was sheared to an average size of ∼500 bp. Tagged proteins were immunoprecipitated with 5 μg mouse anti-Flag (Sigma) or anti-cMyc (Millipore, Bedford, MA) bound to Dynabeads Protein G for immunoprecipitation (Invitrogen). Dynabeads with the immunoprecipitates were washed with dilution buffer [2 mM EDTA (pH 8), 20 mM Tris-HCl (pH 8), 150 mM NaCl, and 1% Triton] twice and washed with wash buffer [2 mM EDTA (pH 8), 20 mM Tris-HCl (pH 8), 150 mM NaCl, 1% Triton, and 0.1% SDS] four times. Protein and cross-linked DNA were eluted in 100 μl of elution buffer (1% SDS and 0.1 M $NaHCO_3$) at 65° for 10 min. To reverse the cross-linking, the mixture was incubated at 65° overnight with 50 μg/ml proteinase K. DNA was extracted with phenol: chloroform:isoamyl alcohol 25:24:1 and precipitated with 5 M NaCl, glycogen, and ethanol. The immunoprecipitates were resuspended in 30 μl of TE [10 mM Tris-Cl (pH 8) and 1 mM EDTA) containing 2 μg/ml RNase cocktail (Ambion). Input DNA was prepared by mixing 20% of the starting lysate (after sonication) with 200 μl TE. The lysate was processed in the same way as the immunoprecipitates, proteinase K was added, the cross-linking was reversed, and the DNA was extracted. The immunoprecipitated DNA and the input were used as templates for quantitative PCR (qPCR) reactions conducted with ABI 7500 instrumentation (Applied Biosystems, Foster City, CA) and SYBR Green PCR Master Mix (Life Technologies). The primers used are listed in Table S3. The results shown represent the average of duplicate biological samples and three technical replicates, and are expressed as percent enrichment of input relative to binding at *ISC1* for Rap1 and Sir3, and percent enrichment relative to binding at the telomere repeats for Abf1, since these are the loci where there is the least binding for each protein and are considered to be the negative controls. The percentage of input was calculated by the percent input method, using the equation 100*2^[adjusted input to 100% − Ct (cycle threshold) (immunoprecipitate)], and the data are presented as the mean ± SD. Statistical analysis was performed using an unpaired two-tailed Student's *t*-test with $P < 0.001$. Statistical significance was calculated for the percent input for each target, compared to the negative control. We also used untagged strains as negative controls calculating the percentage of input (Figure S1).

3C assay

The 3C assay was performed as described in Belton and Dekker (2015b). Briefly, cells were grown in SC medium to an OD_{600} of 1. Cells were fixed with 3% formaldehyde for 20 min at 25°. The cross-linking was quenched by adding 2.5 M glycine at 2× the volume of formaldehyde used in the previous step and the culture was shaken for 5 min at 25°. Cross-linked cells were washed with water and resuspended in the appropriate 1× restriction enzyme buffer. The sample was frozen and ground with liquid nitrogen for 10 min. The ground sample was resuspended in 1× restriction enzyme buffer and adjusted to an OD_{600} of 10. Cells were distributed into a 96-well PCR plate. Chromatin was solubilized by the addition of SDS (0.1% final) and incubated for 10 min at 65°. Triton X-100 was added to a final concentration of 1% to sequester the SDS. Chromatin was digested with 100 units of *Hin*dIII and incubated overnight at 37°. The restriction enzyme was denatured by adding SDS (1.67% final) and incubating for 20 min at 65°. Chromatin fragments were ligated in dilute (12×) conditions, assembling the ligation reaction (1% Triton X-100, 1× ligation buffer, 0.1 mg/ml BSA, 1 mM ATP, 4.8 unit/ml T4 DNA ligase, and water) and incubating for 4 hr at 16°. Cross-links were reversed by incubating the samples for 4 hr at 65° in the presence of 0.0625 mg/ml proteinase K, followed by adding

again 0.0625 mg/ml proteinase K and incubating overnight at 65°. DNA was purified by a series of phenol–chloroform extractions followed by ethanol precipitation. The resulting template was then treated with RNase cocktail (Ambion) and incubated for 1 hr at 37°, yielding the "3C template." In addition to the 3C template, a randomized ligation control template was generated (Belton and Dekker 2015a), which was used to determine the PCR amplification efficiency of specific ligation products. This template was generated by digesting naked, noncross-linked yeast genomic DNA with *Hin*dIII and ligating it in concentrated conditions to maximize the formation of random intermolecular combinations of chimeric ligation products. The resulting template was purified by a series of phenol–chloroform extractions and ethanol precipitations, and treated with RNase cocktail (Ambion).

Once the 3C samples were generated, DNA concentration was determined by SybrGreen qPCR using an internal primer set. 3C samples were adjusted to 50 ng/μl and the concentrations were verified once again by qPCR. Quantification of ligation products was performed with qPCR using Applied Biosystems TaqMan MGB (minor groove binder) probes and PerfeCTa FastMix II Low ROX (carboxy-X-rhodamine compound) (Quanta Biosciences). The qPCR reactions contain an anchor primer (anchor H), a TaqMan probe (probe H), and one of the test primers (primers H1 through H9). The probe and primers used are listed in Table S3. A standard curve was performed with each pair of primers using serial dilutions of a random ligation control (Table S4). The conditions used for qPCR were: 15 min at 95° (cycle 1) and 10 sec at 95°, and 1 min at 60° (cycles 2–40) conducted with ABI 7500 instrumentation (Applied Biosystems). The 3C experiments were performed once for all the strains shown, except for the parental strain with Sil2126 in its natural position, which was performed in two biological replicates. All experiments were done in technical triplicates for each oligonucleotide pair. Data shown in Figure 7 and Figure S8 represent the mean of the three technical replicas and each data point normalized to its standard curve with the random ligation. Statistical analysis was performed using two-way ANOVA with $P < 0.0001$. Statistical significance was calculated by comparing the cross-linking frequencies at each point with the Sil@-32kb strain.

Data availability

All strains and plasmids are available upon request. Strains are listed in Table S1, plasmids in Table S2, and primers in Table S3. Table S4 shows data analysis of the interaction between Sil@-32kb or Sil2126 at its native position and the intergenic regions of telomere E_{-R} by 3C. In addition, there are nine supplementary figures. Supplemental material available at Figshare: https://doi.org/10.25386/genetics.6405983.

Results

Sil2126 requires the telomere E_{-R} context

We have previously identified a *cis*-acting element located in the right telomere of chromosome E (E_{-R}), between *EPA3* and the telomere. This element, called Sil2126, is a 2.126-kb DNA fragment that comprises nucleotide positions 684,673–686,798 (accession number CR380951) (Juárez-Reyes *et al.* 2012). Sil2126 can silence the *URA3* reporter gene integrated at −32 kb in telomere E_{-R} (hereafter called Sil@-32kb). However, it does not display silencing activity in other telomeres at similar distances, suggesting that Sil2126 is only functional in its native telomere (E_{-R}) [Figure 1 and Juárez-Reyes *et al.* (2012)].

The NE is not required for silencing activity when Sil2126 is inserted 32 kb away from telomere E_{-R}

In this subtelomeric region (E_{-R}), there is another *cis*-acting element, the NE, localized 300 bp downstream of the *EPA1* stop codon. The NE negatively regulates *EPA1* expression in a promoter-specific manner and its activity depends on the yKu proteins (Gallegos-García *et al.* 2012). Due to the fact that Sil2126 is only active in this particular subtelomeric region, we decided to test whether the NE is required for Sil@-32kb activity. We used two parental strains, one with Sil@-32kb (Figure 2, line 1) and the second with just the reporter *URA3* (with no Sil@-32kb; Figure 2B, line 2); both constructs were integrated at −32 kb from telomere E_{-R} (Figure 2A). In each of these parental strains, we deleted the NE and tested the silencing level of the reporter. We found that the NE is not required for Sil@-32kb activity when Sil2126 is still at its native position (Figure 2B, compare line 1 with line 3). Even in the absence of both the original copy of Sil2126 (*sil*Δ) and the NE (*ne*Δ), Sil@-32kb is still functional and can silence the reporter (Figure 2B, compare line 5 with line 6). Therefore, the NE is not required for Sil@-32kb activity at the chromosome E_{-R} telomere.

The intergenic region between EPA2 and EPA3, and/or Sil2126 in its original position, are required for Sil@-32kb activity

Since the NE located in the *EPA1-EPA2* intergenic region is not required for Sil@-32kb activity, we wanted to determine whether the intergenic regions between the *EPA* genes at this telomere and the original copy of Sil2126 are responsible for the telomere E_{-R}-specific activity of Sil@-32kb. We replaced the *EPA1-EPA2* and *EPA2-EPA3* intergenic regions with vector sequences maintaining the corresponding genomic distances between the genes and evaluated the Sil@-32kb activity. We tested different combinations of the intergenic region replacements in two backgrounds: a strain lacking Sil2126 (*sil*Δ, Figure 3A, line 1) and a strain with Sil2126 in its original position (Figure 3B, line 1). In the absence of Sil2126 (*sil*Δ), replacement of the *EPA1-EPA2* intergenic region by vector sequences did not have an effect in Sil@-32kb activity (Figure 3A, compare line 1 with line 2). This is consistent with the fact that the NE element is not required for Sil@-32kb activity (Figure 2B, lines 5 and 6). However, replacement of the *EPA2-EPA3* intergenic region in this background resulted in loss of silencing of the reporter by Sil@-32kb (Figure 3A, line 4). As expected, simultaneous replacement of both intergenic regions has the same effect as replacement of only the *EPA2-EPA3* region (Figure 3A, compare line 4 with line 6).

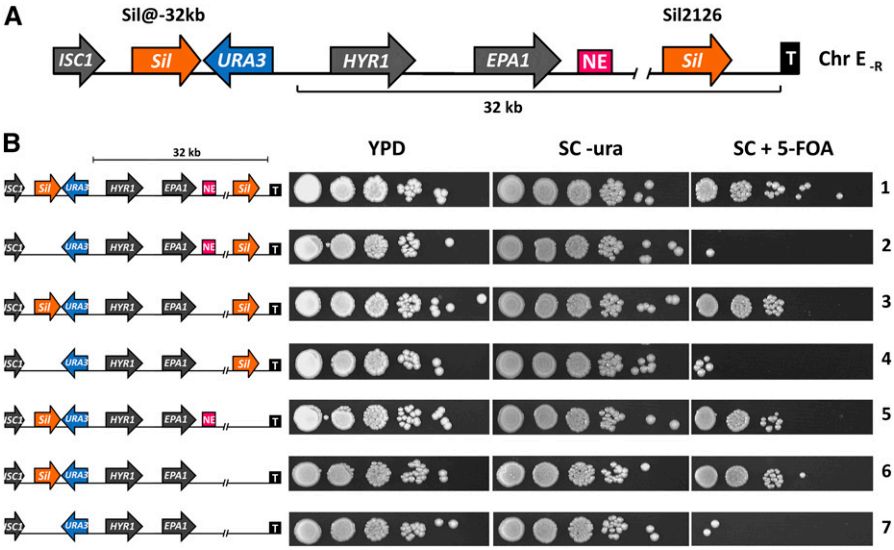

Figure 2 The negative element (NE) is not required for Sil@-32kb activity at the right telomere (T) of chromosome (Chr) E. (A) Schematic representation of Sil@-32kb and the *URA3* reporter integrated in the right T of Chr E (Chr E_{-R}) between the *ISC1* and *HYR1* genes in the parental strain. The NE is shown as a pink square downstream from *EPA1* and Sil2126 is represented as an orange arrow. Note the discontinuity from the NE close to the 3′ UTR of *EPA1* up to the native Sil2126 element near the T. (B) Assessment of the level of silencing of the *URA3* reporter in strains with deletions of *cis*-acting elements (Sil2126 and NE) using a growth plate assay on the indicated media. The genomic structure at the subtelomeric region of T E_R for each strain tested is shown to the left of each line. Note that the insertion of Sil@-32kb generates a duplication of Sil2126 in this region. Lines 1–4 show the silencing activity of Sil@-32kb in the presence or absence of the NE. Lines 5–7 show the silencing activity of derivatives of these strains in which the native copy of Sil2126 has been deleted. Strains were grown to stationary phase in YPD, diluted, and spotted on the media indicated as described in Figure 1B.

In the strain where the original copy of Sil2126 is present, we observed no effect on Sil@-32kb activity when replacing the *EPA1-EPA2* or *EPA2-EPA3* intergenic regions, or simultaneous deletion of both intergenic regions (Figure 3B, compare line 3, line 5 and line 7); that is, Sil@-32kb does not require the *EPA1-EPA2* or *EPA2-EPA3* intergenic regions for silencing of a reporter gene if the original copy is also close to telomere E_{-R}. Taken together, these results indicate that there are *cis*-acting elements present in the *EPA2-EPA3* intergenic region that are required for Sil@-32kb silencing activity. Also, these data suggest that the presence of the original copy of Sil2126 can compensate for the absence of the *EPA2-EPA3* intergenic region elements.

Rap1 and Abf1 putative binding sites are required for Sil@-32kb activity

Sil2126 has several putative binding sites for Rap1 and Abf1, as predicted by the JASPAR 2016 server [Mathelier *et al.* (2016) and Figure 5A], and we have shown that Sil@-32kb activity depends on Rap1 to silence the reporter (Juárez-Reyes *et al.* 2012). In addition, we found that Sil@-32kb activity also depends on Abf1 since, in a strain containing a C-terminal end truncated version of Abf1 (Abf1-43), silencing of the reporter by Sil@-32kb is greatly diminished (Figure S2). This is the first study in which Abf1 has been found to have a role in subtelomeric silencing in *C. glabrata* (L. Castanedo, G. Hernández-Hernández, and I. Castaño, unpublished results). We wondered whether the activity of Sil@-32kb is dependent on the presence of the Rap1 and Abf1 putative binding sites. We tested the level of silencing of the *URA3* reporter in Sil@-32kb precise internal deletions in a *sil*Δ background (Figure 4A). We found that in the absence of the 5′ putative binding sites for Rap1 and Abf1 [*sil* (nt1-262)Δ], Sil@-32kb cannot silence the reporter (Figure 4B, line 3). When we deleted only the putative binding site for Rap1 [*sil* (nt1-204)Δ] but left the putative binding site for Abf1 (Figure 4B line 4), or deleted the putative Abf1 binding site and left the Rap1 putative binding site (Figure 4B, line 5) in the 5′ region of Sil, the level of silencing of the reporter was reduced but was not eliminated (Figure 4B, compare line 1 with lines 4 and 5). In addition, we found that a 334-bp construct containing the combination of just the first binding sites for Rap1 and Abf1 (Sil@-32kb fragment from nt 1–334) cannot mediate the silencing of the reporter, indicating that the other binding sites throughout Sil@-32kb are also required (Figure 4B, line 6).

Rap1 and Sir3 bind to Sil2126 in its original position

To understand the mechanism of action of Sil2126 and whether this element can recruit silencing proteins, in particular Rap1 and Sir3, we performed a ChIP assay using Rap1 tagged with the Flag epitope at the C-terminus and integrated this construct in the native *RAP1* locus (Rap1-Flag, Figure 5A, bottom). We confirmed that the fusion protein is appropriately synthesized by western blotting (Figure S3A) and we determined its functionality by a silencing assay. As shown in Figure S4, the *URA3* reporter was silenced in the strain containing the Rap1-Flag fusion, although at a decreased level compared to the wild-type, untagged strain (Figure S4, lines 2 and 3). We then examined the binding profile of Rap1 at the subtelomeric region of telomere E_{-R} (Figure 5B) by ChIP-qPCR in the parental strain with Sil2126 at its native position. We found that Rap1 is bound only to Sil2126 between the *EPA3* and the telomere, and not elsewhere in this subtelomeric region, except at the telomeric repeats where Rap1 enrichment is very high (Figure 5B, left, columns 4 and 5). In addition, we also determined the distribution of the SIR complex throughout the telomere E_{-R}. We tagged Sir3 at the C-terminal end with the Flag epitope and confirmed that it is expressed and functional (Figures S3A and S4A, line 5), and

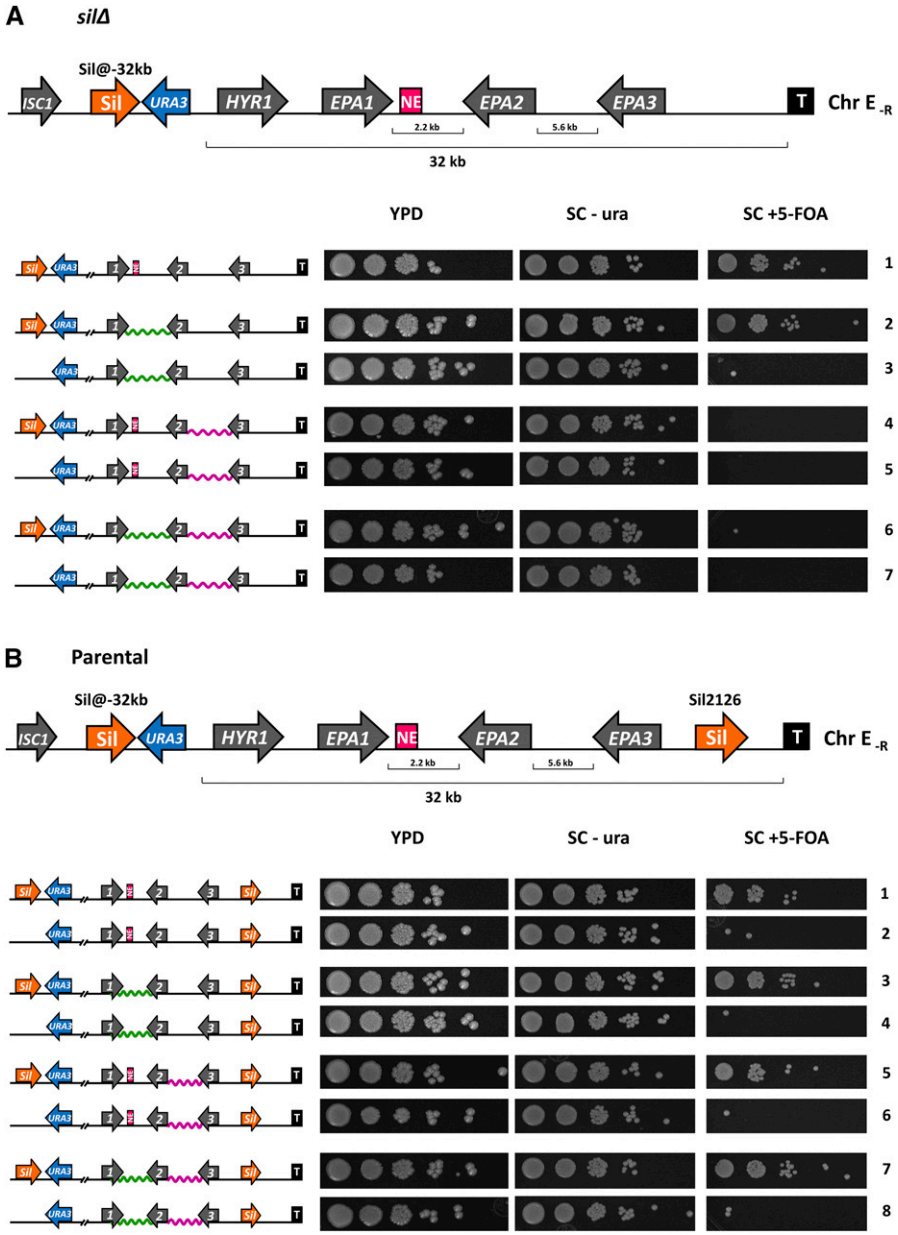

Figure 3 The *EPA2-EPA3* intergenic region is required for Sil@-32kb activity. (A) Top: schematic representation of Sil@-32kb and the *URA3* reporter integrated in the right telomere of chromosome (Chr) E (Chr E_{-R}) between the *ISC1* and *HYR1* genes in the *silΔ* strain. (A) Bottom: silencing activity of Sil@-32kb in strains with a replacement of the *EPA1-EPA2* and *EPA2-EPA3* intergenic regions, and in the absence of the native Sil2126 element. Schematic representation of the genetic structure at telomere (T) E_{-R} in each strain evaluated is shown on the left side. The wavy line represents the replacement of the indicated intergenic region by vector sequences. The distance between genes was maintained. Each strain contains a different combination of the intergenic region replacements. Note the discontinuity from the *EPA1* promoter up to the −32kb region where Sil@-32kb is inserted. (B) Top: Schematic representation of Sil@-32kb and the *URA3* reporter integrated in T E_{-R} between the *ISC1* and *HYR1* genes in the parental strain (note that this strain contains a duplication of Sil2126). Bottom: silencing activity of Sil@-32kb in strains with a replacement of the intergenic regions between *EPA* genes [as in (A), bottom]. The level of silencing in each strain is shown on the right, as assessed by growth on 5-FOA plates as described in Figure 1B. NE, negative element.

then performed ChIP-qPCR assays. In the parental strain, we found that Sir3 is highly enriched at Sil2126 in its original position (Figure S5A, columns 4 and 5), but it is also enriched, albeit to a lesser extent, at longer distances from the telomere, *i.e.*, at the *EPA2-EPA3* intergenic regions and at the NE (Figure S5A, columns 2, 3).

In the absence of Sil2126, Rap1 binding in the intergenic region between EPA2 and EPA3 increases

To determine if the binding profiles of Rap1 and Sir3 are affected by the presence of Sil2126 in this subtelomeric region, we conducted a ChIP assay in the *silΔ* strain (Figure 5C, top). We found that while Rap1 is still highly enriched at the telomere (Figure 5C left column 6), Rap1 binding to a region between *EPA2* and *EPA3* (Figure 5C, left, column 3) is increased when compared to the parental strain with Sil2126 is at its native locus (compare Figure 5B left, column 3 with Figure 5C left, column 3). Instead, Sir3 enrichment throughout this region in the *silΔ* strain did not change significantly compared to the parental strain (compare Figure S5B, columns 2 and 3 with Figure S5A, columns 2 and 3).

Sil2126 can recruit Rap1, Sir3, and Abf1 when inserted 32 kb away from telomere E_R

The subtelomeric region of chromosome E_{-R} contains several putative binding sites for Rap1 and Abf1 (Figure 5A). We have shown that Sil@-32kb activity also depends on Abf1 to silence the reporter (Figure S2). To determine the binding profile of Rap1, Abf1, and Sir3 throughout the subtelomeric region with Sil@-32kb, we analyzed the enrichment of these proteins at several regions in chromosome E_{-R} by ChIP assays. We generated a tagged version of Abf1 at the N-terminal end,

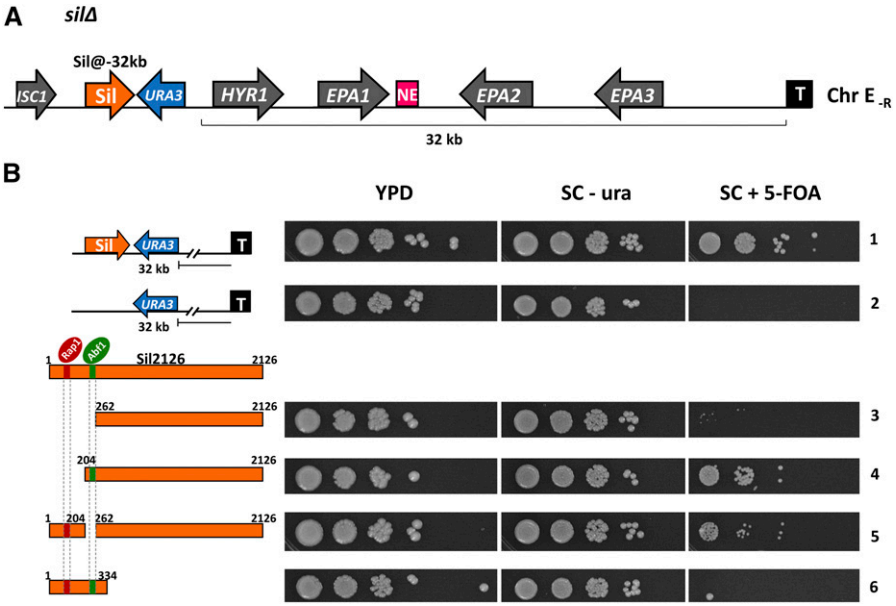

Figure 4 The binding sites for Rap1 and Abf1 are required for Sil@-32kb activity. (A) Schematic representation of Sil@-32kb and the *URA3* reporter integrated in the right telomere (T) of chromosome (Chr) E (Chr E_{-R}), between the *ISC1* and *HYR1* genes in the absence of the original copy of Sil2126 between *EPA3* and the T (*silΔ*). (B) Level of silencing of several Sil2126 deletions of Rap1 and Abf1 putative binding sites. The control strains (Sil@-32kb-*URA3* reporter and only the *URA3* reporter integrated −32 kb from T E_{-R}) are shown in lines 1 and 2. The orange rectangles represent the different deletions of Sil2126. Numbers on the rectangles indicate the end nucleotide position of each version of Sil2126 deletions. All constructs were integrated −32 kb from T E_{-R}. Rap1- and Abf1-binding sites are represented by red and green rectangles, respectively. Equal numbers of cells of each strain were spotted on each media to assess the level of silencing as described in Figure 1B. NE, negative element.

which is expressed from a replicative plasmid under the inducible promoter P_{MT1} (Figure 5A, bottom). We showed that this cMyc-Abf1 fusion protein is expressed (Figure S3B) and functional for silencing (Figure S4B, data not shown). First, we determined by ChIP-qPCR that Abf1 is enriched at the NE, between *EPA1* and *EPA2*, both in the parental strain with Sil2126 at its native locus (Figure 5B, right, column 2) and also in the *silΔ* strain (Figure 5C, right, column 2). We then used the *silΔ* strain with Sil@-32kb (Figure 6A, top) and found that Rap1 is bound to Sil@-32kb (Figure 6A, left, columns 7, 4, and 5), to the *EPA2-EPA3* intergenic region (Figure 6A, left, column 3), and to the region immediately adjacent to the telomeric repeats, as reported for *S. cerevisiae* (Figure 6A, left, column 6). However, Abf1 localization shows a different distribution from that of Rap1. Sil@-32kb can also recruit Abf1 (Figure 6A, right, columns 7, 4, and 5) but, in contrast to Rap1, Abf1 also binds to the NE in this strain (Figure 6A, right, column 2). Sil@-32kb can also recruit Sir3 at that distance from the telomere (Figure S5C, columns 7, 4, and 5). These results show that Rap1, Sir3, and Abf1 are recruited to Sil@-32kb, suggesting that the protosilencer can nucleate a compact chromatin structure at this distance from the telomere to mediate silencing of the reporter.

Sil2126 recruits Rap1 and Abf1 in the absence of the intergenic region between EPA2 and EPA3

Since the *EPA2-EPA3* intergenic region is required for the silencing activity of Sil@-32kb in the absence of the original copy of Sil2126 (Figure 3A, line 4), we decided to determine whether Rap1 and Abf1 can be recruited to Sil@-32kb in a strain where the *EPA2-EPA3* intergenic region has been replaced by vector sequences (Figure 6B, top). The results show that Rap1 and Abf1 are bound at the same positions within Sil@-32kb, even though neither the *EPA2-EPA3* intergenic region nor Sil2126 are present in this strain (Figure 6B). It is noteworthy that the rest of the binding profile of Rap1 and Abf1 throughout this region remains unchanged with respect to the strain that has the native *EPA2-EPA3* intergenic region (compare Figure 6A with Figure 6B), *i.e.*, Rap1 is highly enriched at the telomere (Figure 6A left, column 6) and Abf1 at the NE (Figure 6B right, column 2, and compare Figure 5B with Figure S6A and Figure 5C with Figure S6B). This pattern is also observed in the strain that contains Sil2126 at its native locus (compare Figure S7A with Figure S7B).

A 5′ fragment of Sil2126 (334 bp) efficiently recruits Rap1 and Abf1 when integrated 32 kb away from telomere E_{-R}

We have shown that the 5′ fragment of Sil2126 (334 bp) containing the putative Abf1 and Rap1 binding sites is not sufficient to mediate silencing of the reporter *URA3* (Figure 4B). ChIP assays in the strain containing this 5′ fragment of Sil2126 inserted at −32 kb (Figure 6C, top) showed a strong enrichment of Rap1 and Abf1 binding to this 5′ fragment (Figure 6C, bottom). In contrast, the enrichment of Rap1 in the *EPA2-EPA3* intergenic region is decreased relative to the enrichment at this site in the strain with full-length Sil@-32kb (Figure 6C, left, column 3). The 5′ fragment of Sil recruits Abf1 and Rap1 even more efficiently than the full-length Sil@-32kb, which might suggest that the distribution of Rap1 and Abf1 is rearranged depending on the particular *cis*-acting elements present in this region.

Sil2126 inserted 32 kb away from the telomere interacts with the intergenic region between EPA1 and EPA2 to form a loop and establish silencing

Since Sil@-32kb can silence the adjacent reporter *URA3*, and recruits silencing proteins such as Rap1 and Abf1, we wondered whether a loop can be formed between Sil@-32kb and

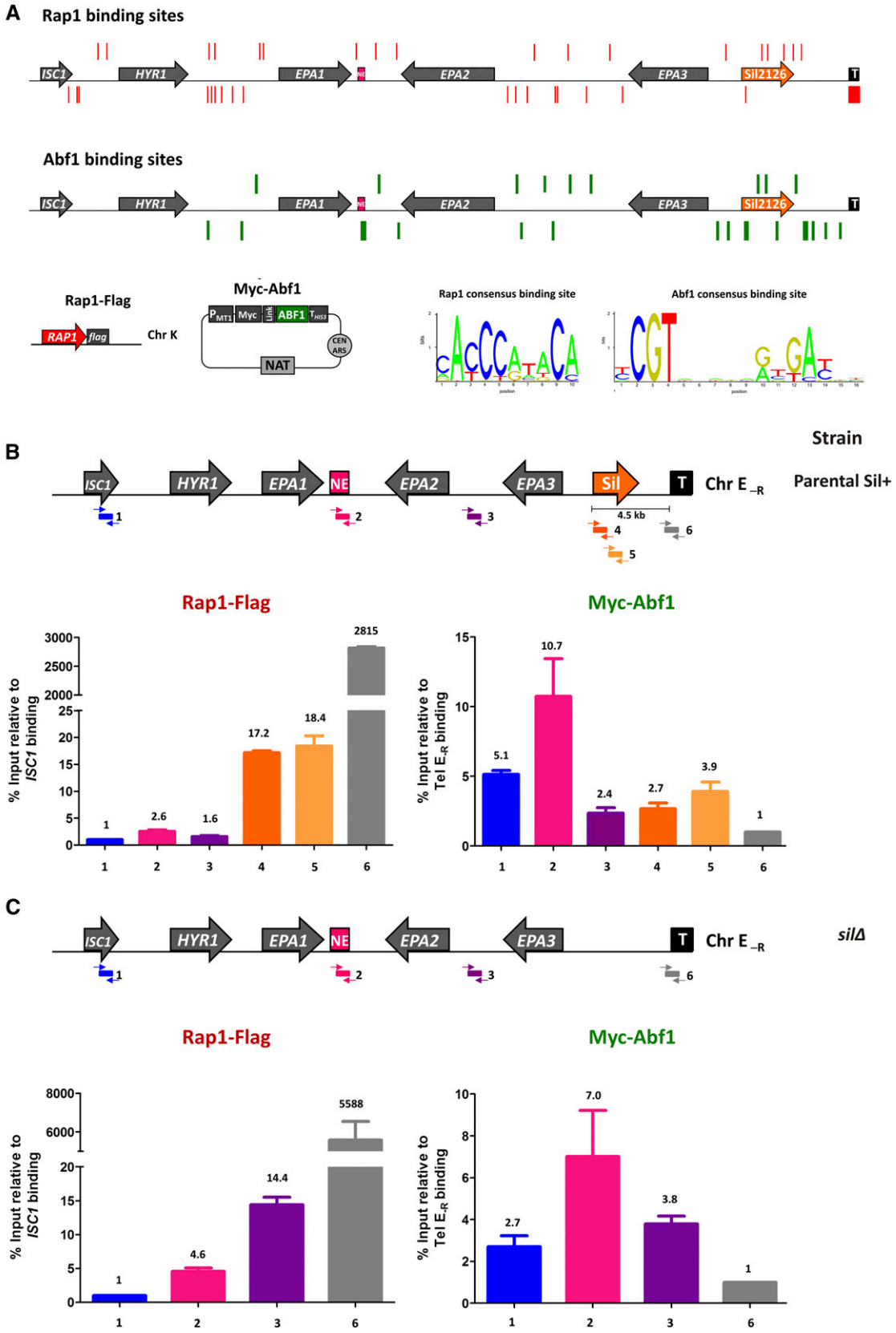

Figure 5 Rap1 and Abf1 are recruited to Sil2126, and at several positions throughout the subtelomeric region of chromosome (Chr) E_{-R}. (A) Top, middle, and bottom right: map of the right telomere (T) of Chr E_{-R} showing Rap1 (red vertical lines) and Abf1 (green vertical lines) putative binding sites. Lines are drawn above or under the map to indicate the DNA strand on which the putative binding sites are localized. Bottom right: we used the

other *cis*-elements in this subtelomeric region, which would allow the propagation of silencing. First, we performed a 3C assay in two strains where the original copy of Sil2126 has been deleted (*sil*Δ); one with Sil@-32kb and the other containing a 3′ fragment of Sil at this position from nt 262–2126 [*sil*(1-262)Δ], which lacks the 5′ end Abf1 and Rap1 putative binding sites, and cannot mediate silencing (Figure 4, line 3). We determined the cross-linking frequency by qPCR using an anchor primer (anchor H) and a Taqman probe (probe H), which anneal at Sil@-32kb (Figure 7A, bottom). We detected a DNA looping interaction between the full-length Sil@-32kb and the *EPA1-EPA2* intergenic region (a 1647-bp fragment that contains the 3′ and downstream region of *EPA1*, including the NE, Figure 7A, purple line). In contrast, the strain with *sil*(nt1-262)Δ did not show any interactions across the subtelomeric region E_{-R} (Figure 7A, green line). These data suggest that Sil@-32kb can induce the formation of a chromatin loop that can propagate silencing. Furthermore, loop formation requires the Rap1 and Abf1 putative binding sites present in the first 262 nt of the protosilencer.

DNA loop formation between Sil@-32kb and the intergenic region between EPA1 and EPA2 depends on silencing proteins

To determine if the interaction observed between Sil@-32kb and the *EPA1-EPA2* intergenic region depends on silencing proteins, we performed a 3C assay using derivative strains from the 3C assay above (*sil*Δ containing Sil@-32kb) but introducing either the *rap1-21* allele, which is a deletion of the last 21 amino acids of Rap1 and is completely defective for silencing, or the *sir3*Δ allele (Table S1). We found that the interaction between Sil2126 and the *EPA1-EPA2* intergenic region is lost in the absence of the silencing activity of Rap1 (*rap1-21*Δ) or Sir3 (*sir3*Δ) (Figure 7A, red line and Figure S8, blue line). These data suggest that at least Rap1 and Sir3 silencing proteins are necessary for the interaction between these two loci, possibly by favoring a compact structure through protein–protein interactions.

Sil2126 in its native position interacts with the region between EPA2 and EPA3

We next asked whether Sil2126 in its native position is able to interact with the elements that are required for its activity at −32 kb. We performed a 3C assay to determine the cross-linking frequencies in the parental strain where Sil2126 is in its native position using the anchor primer H and the Taqman probe (probe H) aligned within Sil2126 (Figure 7B, bottom). We detected a strong interaction between Sil2126 and the *EPA2-EPA3* intergenic region (primers H7 and H8). This is in agreement with our previous data in which Sil@-32kb requires the *EPA2-EPA3* intergenic region for its silencing activity. In addition, we observed weaker interactions between Sil2126 with the flanking intergenic regions of *EPA1* (Figure 7B). These data suggest that the subtelomeric region of chromosome E_{-R} is able to form different three-dimensional structures between the various *cis*-acting elements.

Formation of a DNA loop between Sil@-32kb and the region between EPA1 and EPA2 results in repression of the EPA1 promoter

Since Sil@-32kb forms a loop with the region downstream from *EPA1*, and this loop allows the propagation of silencing up to 32 kb away from the telomere, we wondered whether this interaction allows a heterochromatin structure that would result in repression of *EPA1*, which forms part of this loop. To test this, we measured activity of the *EPA1* promoter using a transcriptional fusion of P_{EPA1} with *GFP* by flow cytometry in a strain that only contains Sil@-32kb. We have previously shown that dilution of cells into fresh media from stationary phase cultures results in the induction of *EPA1*. We used stationary phase cultures diluted into fresh media and found that *GFP* could not be induced under this condition, which results in *EPA1* induction in the strain that does not contain Sil@-32kb (Figure 8). These data suggest that Sil@-32kb forms a three-dimensional structure that does not allow the induction of P_{EPA1} upon dilution into fresh medium.

Discussion

Members of a large family of cell wall protein genes called the *EPA* family, some of which have been shown to function as adhesins (*EPA1*, *EPA6*, and *EPA7*) (Cormack *et al.* 1999; De Las Peñas *et al.* 2003; Castaño *et al.* 2005), are encoded in the subtelomeric regions of chromosomes of the fungal pathogen *C. glabrata*. In the BG2 strain background (Cormack and

indicated *S. cerevisiae* consensus binding sites for Rap1 and Abf1 to predict the putative binding sites in *C. glabrata* using the JASPAR 2016 server. Bottom left: schematic representation of the tagged versions of Rap1 and Abf1 used for chromatin immunoprecipitation (ChIP) experiments. Rap1 was fused with the Flag epitope at the C-terminal end and the wild-type allele was replaced by the tagged version in its original chromosomal location. The Abf1 construct is provided on a replicative plasmid in which Abf1 is fused to the c-Myc epitope at the N-terminal end. The fusion is driven by the inducible promoter P_{MT1}, which is induced in the presence of copper. (B and C) Rap1 is recruited by Sil2126 at its native position and/or propagated from the T. Top: schematic representation of Chr E_{-R} indicating the regions tested in the ChIP assay. Each amplified fragment with the corresponding primer set is numbered and the numbers correspond to each bar in the graph; the arrows indicate the position where the quantitative PCR (qPCR) primers anneal. The distance from Sil2126 to the T is indicated. Bottom: Rap1-Flag and cMyc-Abf1 enrichment is represented as percentage of input relative to binding at *ISC1* for Rap1 or at the telomere repeats for Abf1. Each column corresponds to the regions amplified by qPCR, represented in the Chr E_{-R} map as numbered rectangles. The number of each primer set indicates the same region amplified across the different strains. The percentage of input was calculated by percent input method using the equation 100*2^[adjusted input to 100% - Ct (cycle threshold) (immunoprecipitate)]. (B) ChIP assay in the parental strain (Sil2126 in its original position). (C) ChIP assay in a *sil*Δ strain. NE, negative element.

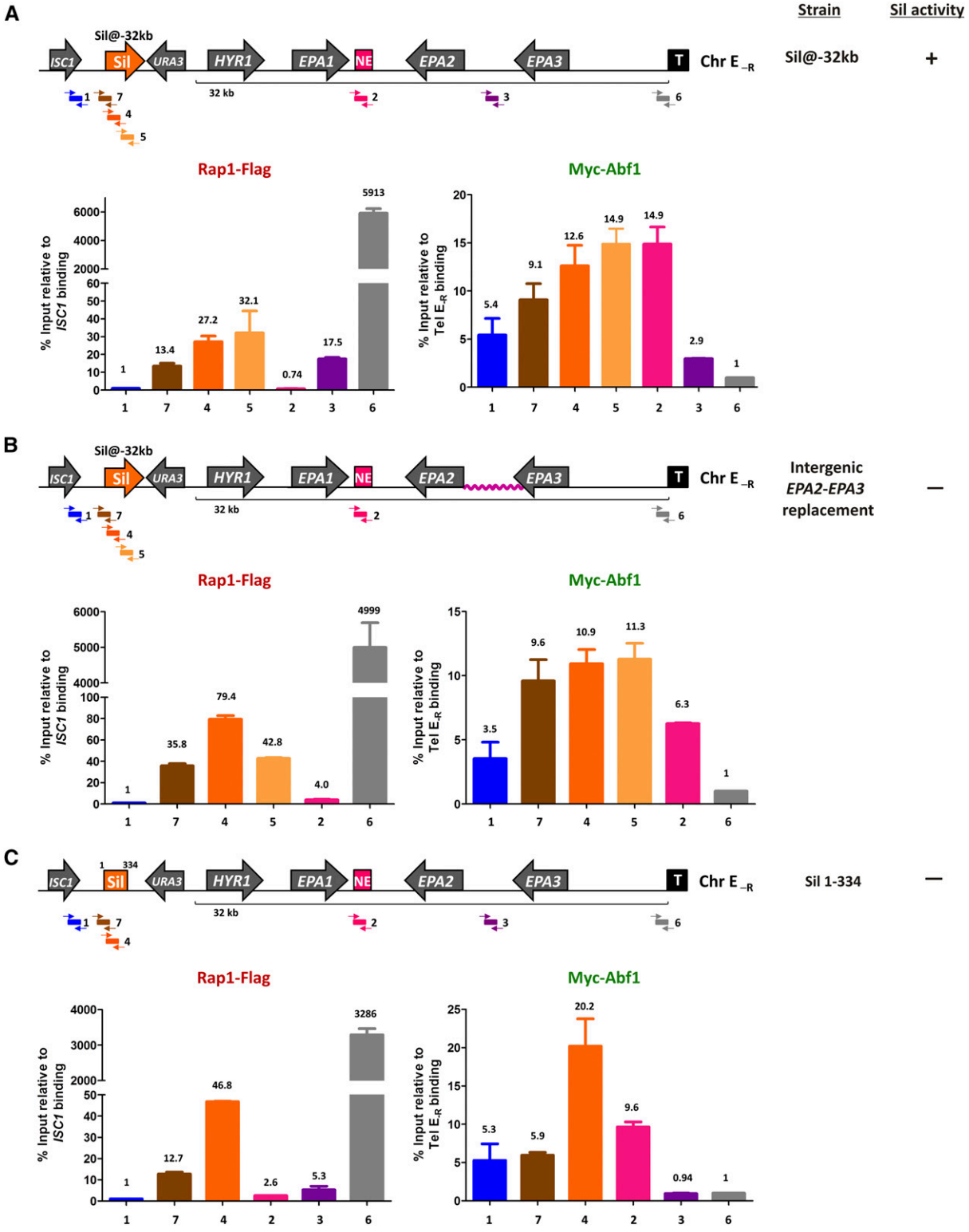

Figure 6 Sil2126 can recruit Rap1 and Abf1 when inserted 32 kb away from the telomere (T). (A) Sil@-32kb can recruit Rap1 and Abf1. Top: schematic representation of the subtelomeric region of chromosome (Chr) E_{-R} in the strain where the original copy of Sil2126 is deleted and the Sil@-32kb-*URA3* reporter is inserted at Chr E_{-R}. The position of the fragments amplified with the indicated primer sets for the chromatin immunoprecipitation assays is indicated below the map. Each amplified fragment with the corresponding primer set is numbered, and the numbers correspond to each bar in the graphs in all panels and to Figure 5. Bottom: Rap1-Flag and cMyc-Abf1 enrichment represented as percentage of input relative to binding at *ISC1* for Rap1 or at the T repeats for Abf1, which was calculated as described in Figure 5B. (B) Rap1-Flag and cMyc-Abf1 are recruited at −32 kb in the absence of the *EPA2-EPA3* intergenic region. Top: schematic representation of Chr E_{-R} in the absence of the original copy of Sil2126 and with a replacement of the *EPA2-EPA3* intergenic region by vector sequences (represented by the wavy line). The regions tested are indicated as described for (A) and

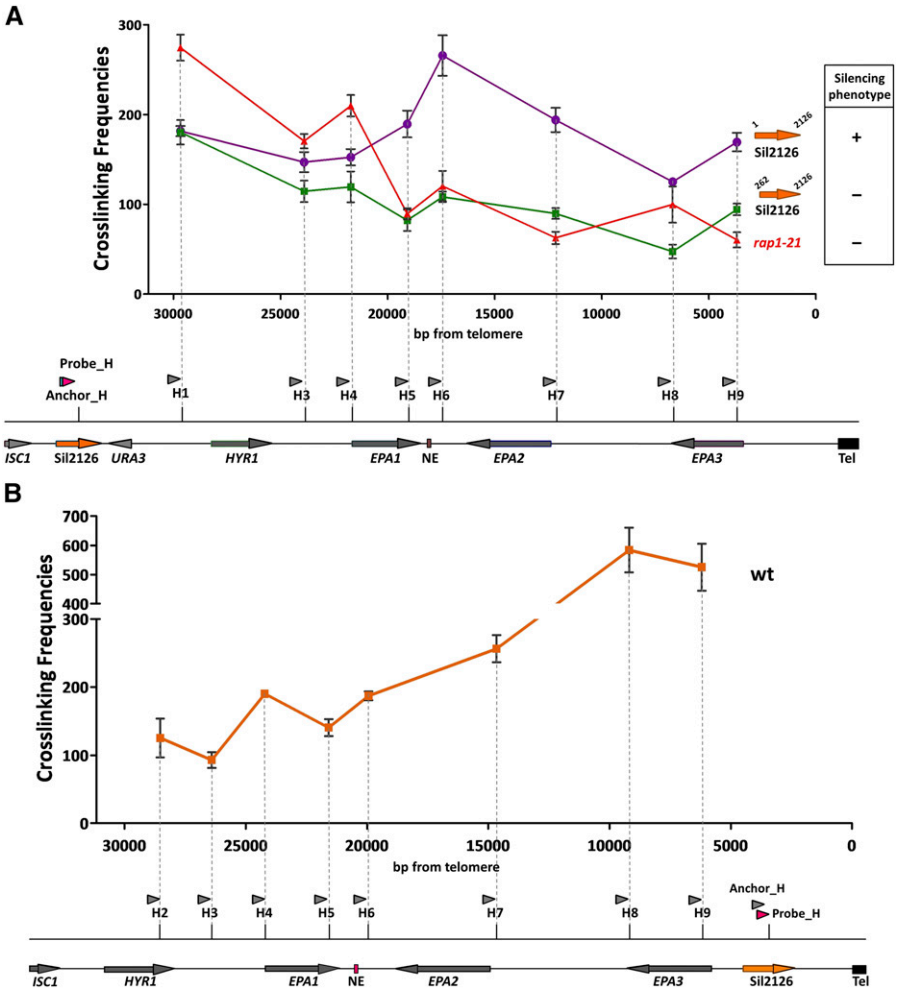

Figure 7 Sil2126 placed at −32 kb interacts with a fragment downstream of *EPA1* to propagate silencing, and Sil2126 in its native position interacts with the *EPA2-EPA3* intergenic region. (A) Top: chromosome (Chr) conformation capture (3C) analysis represented by cross-linking frequencies throughout the Chr E_{-R} in derivatives of the *sil*Δ strain. Each point in the graph represents the cross-linking frequency of each *Hin*dIII fragment tested in the different locations across the subtelomeric region. The cross-linking frequencies in a strain with Sil@-32kb is represented by the purple line, the strain with the deletion construct [*sil*(*1-262*)Δ] inserted at −32 kb is represented by the green line, and the *rap1-21* strain is represented by the red line. The silencing activity of these constructs is indicated. (A) Bottom: schematic representation of the telomere (Tel) E_{-R} with the Sil@-32kb and the *URA3* reporter inserted at −32 kb. The arrowheads above the map represent the primers used in combination with the anchor H and the TaqMan probe H located in Sil2126 (also indicated as blue and pink arrowheads, respectively). The digestion sites of the restriction enzyme (*Hin*dIII) are indicated (H1–H9). (B) Top: 3C analysis shown as cross-linking frequencies throughout Chr E_{-R} in the parental strain with Sil2126 at is native locus. Each point in the graph represents the cross-linking frequency of each *Hin*dIII fragment tested in the different locations across the subtelomeric region. The cross-linking frequencies in the parental strain with Sil2126 at its native locus are represented by the orange line. Bottom: schematic representation of the telomere E_{-R} in the parental strain. The arrowheads above the map represent the primers used in combination with the anchor H and the TaqMan probe H located in Sil2126 (also indicated as blue and pink arrowheads, respectively). The location and numbers of the primers correspond to the primers in (A). Note that the *y*-axis is discontinuous.

Falkow 1999), the expression of most of the *EPA* genes is repressed by chromatin-based silencing due to their localization near the telomeres. In particular, *EPA1*, which encodes the major adhesin in *C. glabrata* and is localized ± 20 kb from the telomere E_{-R}, is tightly regulated by several layers of regulation, including subtelomeric silencing (Gallegos-García *et al.* 2012). The presence of telomere-specific *cis*-acting elements might explain the significant differences found in the requirement for some silencing proteins at different telomeres, which result in the complex and unique transcriptional regulation of native subtelomeric genes. For example, *EPA1* at the telomere E_{-R} is subject to promoter-specific repression independent of the subtelomeric silencing, which is mediated by a *cis*-acting element called the NE (Gallegos-García *et al.* 2012). In addition to the NE, telomere E_{-R} contains the *cis*-acting Sil2126 protosilencer between *EPA3* and the telomere repeats, which contributes to silencing of the *EPA* genes present at this region.

In this work, we showed that the protosilencer Sil2126 can recruit silencing proteins, such as Rap1, Sir3, and Abf1, both when present at its native position or when inserted 32 kb away from the telomere. We propose that Sil2126 can induce the formation of a DNA loop in this subtelomeric region by interacting with an intergenic region in the *EPA1-3* cluster, probably through protein–protein interactions between silencing proteins recruited to Sil2126 and the intergenic regions involved. This results in remodeling of the chromatin structure close to the telomere E_R leading to the formation of heterochromatin.

correspond to the bars in the graph. Bottom: Rap1-Flag and cMyc-Abf1 enrichment represented as percentage of input, as in Figure 5B. (C) There is a higher enrichment of Rap1-Flag and cMyc-Abf1 when a 5′ fragment of Sil2126 (334 bp) containing the putative Abf1- and Rap1-binding sites is integrated at −32 kb. Top: schematic representation of the subtelomeric region of Chr E_{-R} in the strain in which a 334-bp fragment from the 5′ end of Sil2126 was inserted at −32 kb, followed by the *URA3* reporter. The regions tested by qPCR are indicated as described for (A) and correspond to the bars in the graph. Bottom: Rap1-Flag and cMyc-Abf1 enrichment is represented as percentage of input, as described in Figure 5B. NE, negative element.

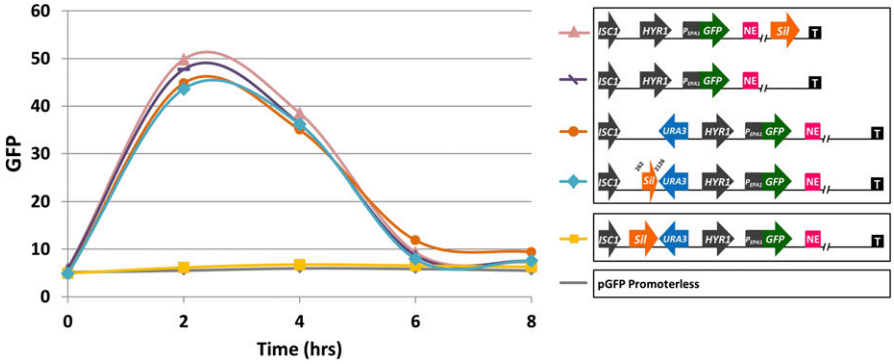

Figure 8 *EPA1* expression is not induced when Sil@-32kb and the *URA3* reporter are placed −32 kb from the T E_{-R}. Activity of the *EPA1* promoter as measured by FACS. Strains were grown in SC medium supplemented with 25 mg/liter uracil for 48 hr at 30°. Cells were diluted into fresh medium and samples were taken every 2 hr. Schematic representation of the genetic structure at telomere E_{-R} in each strain evaluated is shown on the right side. Figure S9 shows the histograms corresponding to the last strain in the graph. NE, negative element; T, telomere.

Cis-acting elements present in the intergenic region between EPA2 and EPA3 are required for Sil2126 at −32 kb

We have previously shown that the protosilencer Sil@-32kb is only functional in its native telomere (Juárez-Reyes *et al.* 2012), and in this work we found that in the absence of the native copy, it requires *cis*-acting elements located in the *EPA2-EPA3* intergenic region, but not the NE or the entire *EPA1-EPA2* intergenic region, for its activity (Figure 3A, line 4). The *EPA2-EPA3* region contains several putative binding sites for Rap1 and Abf1 (Figure 5A), which could have a role in the spreading of silencing at the subtelomere E_{-R} to up to 20 kb. Since it is thought that silencing can propagate by the formation of loops between silencers and protosilencers, or between distant protosilencers (Lebrun *et al.* 2001; Fourel *et al.* 2002), Sil2126 and the *cis*-acting elements in the *EPA2-EPA3* intergenic region could work synergistically to extend silencing. This could explain the specificity of Sil2126 for the E_{-R} telomere. Sil2126 in its native locus can compensate for the absence of the *EPA2-EPA3* intergenic region (compare Figure 3A, line 4 with Figure 3B, line 5), probably because Sil2126 recruits silencing proteins and both copies of Sil2126 could interact through protein–protein interactions.

Rap1, Abf1, and Sir3 bind at several positions throughout the subtelomeric region of chromosome E_{-R}, and are recruited to Sil2126 when inserted 32 kb away from the telomere E_{-R}

In this work, we showed that Sir3 and Rap1 are clearly bound to Sil2126 at its native position, close to the telomere (Figure 5B, left and Figure S5A). Furthermore, this protosilencer can recruit Rap1, Sir3, and Abf1 when inserted in a silencing-free environment (32 kb away from the telomere; Figure 6A and Figure S5C). These results suggest that the mechanism of silencing of Sil2126 is through the recruitment of Rap1 and Abf1. In turn, these proteins recruit the SIR complex to establish a silent domain in a similar way to the interactions between Rap1 with Sir3 and Sir4 reported in *S. cerevisiae* (Moretti *et al.* 1994; Cheng and Gartenberg 2000; Moretti and Shore 2001). Rap1 and/or Abf1 could bind to the *cis*-acting elements with different affinities or even cooperatively, so that the equilibrium could be driven toward the formation of a compact silent chromatin structure.

Sil2126 at its natural position strongly interacts with the intergenic region between EPA2 and EPA3

In its normal context between *EPA3* and the telomere, Sil2126 strongly interacts with the *EPA2-EPA3* intergenic region (Figure 7B, orange line) resulting in a loop that is shown schematically in Figure 9B. We propose that in the parental strain, Sil2126 can in fact form alternative loops with *cis*-acting elements across the subtelomeric region E_{-R}. The most frequent loop is with the *EPA2-EPA3* intergenic region, but also to a lesser extent, a loop can be formed with the NE region. We think that this compact structure results in the strong repression of *EPA3*, *EPA2*, and also *EPA1* observed in the parental strain under most *in vitro* conditions (Castaño *et al.* 2005; Gallegos-García *et al.* 2012). Another possibility is that the strong signal detected between Sil2126 and its immediate vicinity (Figure 7B, probes H8 and H9) could be due to an alternative chromatin conformation at this site, and not to a loop *per se*.

Sil@-32kb propagates silencing by interacting with the intergenic region between EPA1 and EPA2

We showed that the *cis*-acting element Sil@-32kb (in the *silΔ* strain) interacts with a fragment in the *EPA1-EPA2* intergenic region between *EPA1* and *EPA2* through formation of a DNA loop (Figure 7, purple line). This interaction is significantly more frequent than with any other fragment in this subtelomeric region in the absence of Sil at its native position, and thus suggests that the interaction is specific. Importantly, we showed that loop formation in this strain critically depends on both Rap1 and Sir3 (Figure 7A, red line and Figure S8, blue line). Besides, the deletion of the first 262 bp of Sil2126, which contain the 5′ end Rap1 and Abf1-binding sites, results in the loss of this interaction (Figure 7, green line). The loop formation allows the propagation of silencing up to 32 kb away from the telomere, and forms a heterochromatin domain that includes *EPA1* as assessed by the lack of induction of the P_{EPA1} upon dilution of stationary phase cells into fresh medium (Figure 8). It should be pointed out that the fragment that interacts with Sil@-32kb contains the NE, and we showed that the NE is not required for Sil@-32kb activity (Figure 2). It is possible that when Sil2126 is inserted at −32 kb, it can also promote less-strong interactions with another *cis*-acting element, possibly the *EPA2-EPA3*

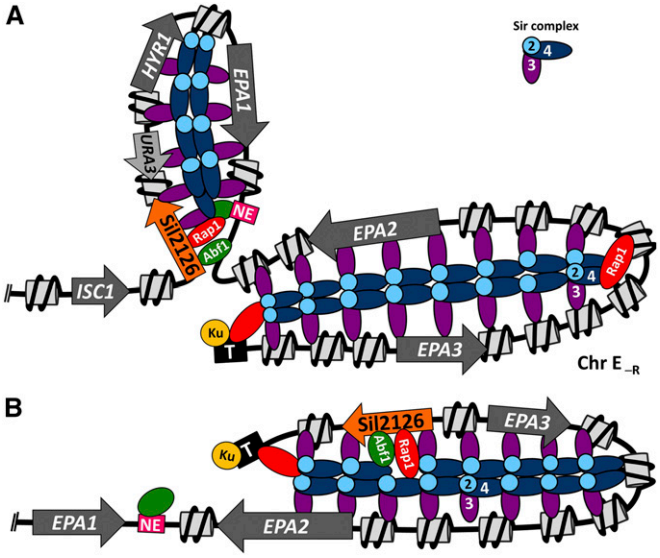

Figure 9 Models for alternative silenced superstructures formed in two strains: a *sil*Δ strain with a *cis*-acting element Sil2126 inserted at −32 kb (Sil@-32kb) and in the parental strain with Sil2126 at its native position. (A) Proposed DNA loops formed in the *sil*Δ strain with Sil@-32kb. The protosilencer Sil@-32kb and the *EPA1-EPA2* intergenic region interact to form a loop. This structure is probably formed through the interaction between different silencing proteins—Rap1, Abf1, and the SIR complex—to maintain a silenced superstructure. The silencing can propagate up to 32 kb due to the presence of Sil2126 at this position, which presumably would act by recruiting Rap1 and Abf1 proteins. The SIR complex is represented by: light blue circles (Sir2), purple ovals (Sir3), and dark blue ovals (Sir4). Rap1 is represented as red ovals, the Ku proteins (yKu70 and yKu80) are represented as a yellow circle, and Abf1 as green ovals. *EPA* genes are represented as gray arrows and Sil2126 as an orange arrow. The model shows another proposed loop formed between the telomere and the NE in this strain. This loop is inferred from genetic data showing that silencing from the telomere directly affects *EPA1* expression (Gallegos-García *et al.* 2012). (B) Proposed chromatin loop formed between Sil2126 at is native position and the *cis*-acting elements in the *EPA2-EPA3* intergenic region in the parental strain. Silencing proteins are represented in the same way as (A). Chr, chromosome; NE, negative element.

intergenic region. We speculate that this proposed, less-frequent loop between the Sil@-32kb and *EPA2-EPA3* intergenic region might be more efficient at silencing the reporter integrated with Sil@-32kb. We think that this is possible because replacement of the *EPA2-EPA3* intergenic region, and therefore loss of this alternate loop with the *EPA2-EPA3* intergenic region, completely abolishes silencing of *URA3* (Figure 3A, line 4). Recently, 3C assays have been used to find potentially new *cis*-acting elements (Liu and Garrard 2005), and we are currently testing other regions of interaction using different oligonucleotides throughout this region.

The proteins involved in bridging interactions between these *cis*-acting elements might be the SIR complex recruited by Rap1 and Abf1 bound to Sil2126. It is thought that to attain a repressed domain, the SIR complex bound to nucleosomes needs to compact the chromatin into a higher-order structure, probably by folding the telomere and generating a compact domain. Interactions at a distance between silencers or protosilencers, and the nucleation sites like the telomeres, could promote the initial recruitment of the SIR complex or the maintenance of the compact silent chromatin (Kueng *et al.* 2013; Thurtle and Rine 2014). Indeed, in the heterochromatin regions in *S. cerevisiae* like the mating loci, silencer elements (*HMR-E* and *HMR-I*) can interact with each other to silence *HMR* and the SIR complex is required (Valenzuela *et al.* 2008; Miele *et al.* 2009).

We propose that a three-dimensional structure is necessary for spreading of the subtelomeric silencing, and requires a repertoire of *cis*-acting elements and silencing proteins bound to these elements (Figure 9A). When Sil2126 is integrated 32 kb away from the telomere in a *sil*Δ background, we propose a model where Sil@-32kb can induce the formation of a loop in this subtelomeric region by interacting with an *EPA1-EPA2* intergenic region, probably through protein–protein interactions between silencing proteins recruited to Sil2126 and the intergenic region involved. This results in remodeling of the chromatin structure close to the telomere E_R, leading to the formation of heterochromatin and the spreading of silencing. In fact, it is possible that there are alternate loops that can be formed between Sil2126 (at its native position or at −32 kb) and the various *cis*-acting elements throughout this region. This, in turn, depends on the binding of Rap1 and Abf1, and the subsequent recruitment of the SIR complex. The nucleation mechanisms of the SIR complex at increasing distances from the telomere are not known, and might be achieved by propagating from the telomeric repeats recruited by Rap1 and/or from the other *cis*-elements that bind Rap1. In this regard, it is interesting to note that Rap1 can associate with distal sites and loop out intervening DNA (Hofmann *et al.* 1989). This model is supported by the recent finding in *S. cerevisiae* that the spreading of the SIR complex on chromatin is through pairs of nucleosomes lacking histone H4K16 acetylation and H3K79 methylation, and that this propagation can occur across nonneighboring nucleosomes, which can promote loop formation in the heterochromatin (Behrouzi *et al.* 2016).

The fact that most of the *EPA* genes are located in subtelomeric regions and regulated by subtelomeric silencing, at least in some strains of *C. glabrata*, would seem to imply that all *EPA* genes are regulated in a similar way. However, each telomere contains different *cis*-acting elements and different requirements for silencing proteins, and this allows for flexibility in the regulation of individual *EPA* genes, which would allow the cell to respond to different environmental conditions by expressing the appropriate *EPA* gene for each host niche.

Acknowledgments

We thank Verónica Zárate and the Laboratorio Nacional de Biotecnología Agrícola, Médica y Ambiental (LANBAMA) for expert technical assistance with sample sequencing, and Nicolás Gómez for excellent technical assistance with the chromatin immunoprecipitation assay. E.L.-F., G.H.-H., and

L.C. were supported by Consejo Nacional de Ciencia y Tecnología (CONACyT) fellowship numbers 261740, 590366, and 448801, respectively. This work was supported by CONACyT grant number CB-2014-239629 to I.C.

Author contributions: E.L.-F. and I.C. designed and performed the experiments and wrote the manuscript. G.H.-H. and L.C. tagged the Rap1 and Abf1 proteins. G.G.-E. gave technical assistance. K.O. supervised the 3C experiments. A.D.L.P. edited the manuscript. All authors were involved in the final preparation of the manuscript.

Literature Cited

Andrulis, E. D., A. M. Neiman, D. C. Zappulla, and R. Sternglanz, 1998 Perinuclear localization of chromatin facilitates transcriptional silencing. Nature 394: 592–595. https://doi.org/10.1038/29100

Ausubel, , F. M., R. Brent, R. E. Kingston, D. D. Moore, and J. G. Seidman *et al.*, (Editors) 2001 *Current Protocols in Molecular Biology*. John Wiley & Sons, Hoboken, NJ.

Baur, J. A., Y. Zou, J. W. Shay, and W. E. Wright, 2001 Telomere position effect in human cells. Science 292: 2075–2077. https://doi.org/10.1126/science.1062329

Behrouzi, R., C. Lu, M. Currie, G. Jih, N. Iglesias *et al.*, 2016 Heterochromatin assembly by interrupted Sir3 bridges across neighboring nucleosomes. Elife 5: e17556. https://doi.org/10.7554/eLife.17556

Belton, J.-M., and J. Dekker, 2015a Randomized ligation control for chromosome conformation capture. Cold Spring Harb. Protoc. 2015: 587–592. https://doi.org/10.1101/pdb.prot085183

Belton, J.-M., and J. Dekker, 2015b Chromosome conformation capture (3C) in budding yeast. Cold Spring Harb. Protoc. 2015: 580–586. https://doi.org/10.1101/pdb.prot085175

Bonev, B., and G. Cavalli, 2016 Organization and function of the 3D genome. Nat. Rev. Genet. 17: 661–678 (erratum: Nat. Rev. Genet. 17: 772). https://doi.org/10.1038/nrg.2016.112

Castano, I., R. Kaur, S. Pan, R. Cregg, A. De, Las Penas *et al.*, 2003 Tn7-based genome-wide random insertional mutagenesis of Candida glabrata. Genome Res. 13: 905–915. https://doi.org/10.1101/gr.848203

Castaño, I., S.-J. Pan, M. Zupancic, C. Hennequin, B. Dujon *et al.*, 2005 Telomere length control and transcriptional regulation of subtelomeric adhesins in Candida glabrata. Mol. Microbiol. 55: 1246–1258. https://doi.org/10.1111/j.1365-2958.2004.04465.x

Cheng, T. H., and M. R. Gartenberg, 2000 Yeast heterochromatin is a dynamic structure that requires silencers continuously. Genes Dev. 14: 452–463. https://doi.org/10.1101/gad.14.4.452

Cormack, B. P., and S. Falkow, 1999 Efficient homologous and illegitimate recombination in the opportunistic yeast pathogen Candida glabrata. Genetics 151: 979–987. https://doi.org/10.1073/PNAS.94.14.7412

Cormack, B. P., N. Ghori, and S. Falkow, 1999 An adhesin of the yeast pathogen Candida glabrata mediating adherence to human epithelial cells. Science 285: 578–582. https://doi.org/10.1126/science.285.5427.578

De Las Peñas, A., S. J. Pan, I. Castaño, J. Alder, R. Cregg *et al.*, 2003 Virulence-related surface glycoproteins in the yeast pathogen Candida glabrata are encoded in subtelomeric clusters and subject to RAP1- and SIR-dependent transcriptional silencing. Genes Dev. 17: 2245–2258. https://doi.org/10.1101/gad.1121003

Domergue, R., I. Castaño, A. De Las Peñas, M. Zupancic, V. Lockatell *et al.*, 2005 Nicotinic acid limitation regulates silencing of Candida adhesins during UTI. Science 308: 866–870. https://doi.org/10.1126/science.1108640

Duan, Z., M. Andronescu, K. Schutz, S. McIlwain, Y. J. Kim *et al.*, 2010 A three-dimensional model of the yeast genome. Nature 465: 363–367. https://doi.org/10.1038/nature08973

Ellahi, A., D. M. Thurtle, and J. Rine, 2015 The chromatin and transcriptional landscape of native Saccharomyces cerevisiae telomeres and subtelomeric domains. Genetics 200: 505–521. https://doi.org/10.1534/genetics.115.175711

Fourel, G., E. Revardel, K. Catherine Elaine, and E. Gilson, 1999 Cohabitation of insulators and silencing elements in yeast subtelomeric regions. EMBO J. 18: 2522–2537. https://doi.org/10.1093/emboj/18.9.2522

Fourel, G., E. Lebrun, and E. Gilson, 2002 Protosilencers as building blocks for heterochromatin. BioEssays 24: 828–835. https://doi.org/10.1002/bies.10139

Gallegos-García, V., S.-J. Pan, J. Juárez-Cepeda, C. Y. Ramírez-Zavaleta, M. B. Martin-del-Campo *et al.*, 2012 A novel downstream regulatory element cooperates with the silencing machinery to repress EPA1 expression in Candida glabrata. Genetics 190: 1285–1297. https://doi.org/10.1534/genetics.111.138099

Gardner, M. J., N. Hall, E. Fung, O. White, M. Berriman *et al.*, 2002 Genome sequence of the human malaria parasite Plasmodium falciparum. Nature 419: 498–511. https://doi.org/10.1038/nature01097

Gartenberg, M. R., and J. S. Smith, 2016 The nuts and bolts of transcriptionally silent chromatin in Saccharomyces cerevisiae. Genetics 203: 1563–1599. https://doi.org/10.1534/genetics.112.145243

Gotta, M., T. Laroche, A. Formenton, L. Maillet, H. Scherthan *et al.*, 1996 The clustering of telomeres and colocalization with Rap1, Sir3, and Sir4 proteins in wild-type Saccharomyces cerevisiae. J. Cell Biol. 134: 1349–1363. https://doi.org/10.1083/jcb.134.6.1349

Gottschling, D. E., O. M. Aparicio, B. L. Billington, and V. A. Zakian, 1990 Position effect at S. cerevisiae telomeres: reversible repression of Pol II transcription. Cell 63: 751–762. https://doi.org/10.1016/0092-8674(90)90141-Z

Guo, B., C. A. Styles, Q. Feng, and G. R. Fink, 2000 A Saccharomyces gene family involved in invasive growth, cell – cell adhesion, and mating. Proc. Natl. Acad. Sci. USA 97: 12158–12163. https://doi.org/10.1073/pnas.220420397

Hediger, F., F. R. Neumann, G. Van Houwe, K. Dubrana, and S. M. Gasser, 2002 Live imaging of telomeres: yKu and Sir proteins define redundant telomere-anchoring pathways in yeast. Curr. Biol. 12: 2076–2089. https://doi.org/10.1016/S0960-9822(02)01338-6

Hofmann, J. F. X., T. Laroche, A. H. Brand, and S. M. Gasser, 1989 RAP-1 factor is necessary for DNA loop formation in vitro at the silent mating type locus HML. Cell 57: 725–737. https://doi.org/10.1016/0092-8674(89)90788-5

Horn, D., and A. M. Cross, 1995 A developmentally regulated position effect at a telomeric locus in Trypanosoma brucei. Cell 83: 555–561. https://doi.org/10.1016/0092-8674(95)90095-0

Juárez-Reyes, A., C. Y. Ramírez-Zavaleta, L. Medina-Sánchez, A. De Las Peñas, and I. Castaño, 2012 A protosilencer of subtelomeric gene expression in Candida glabrata with unique properties. Genetics 190: 101–111. https://doi.org/10.1534/genetics.111.135251

Keely, S. P., H. Renauld, A. E. Wakefield, M. T. Cushion, A. G. Smulian *et al.*, 2005 Gene arrays at Pneumocystis carinii telomeres. Genetics 170: 1589–1600. https://doi.org/10.1534/genetics.105.040733

Klevay, M. J., D. L. Horn, D. Neofytos, M. A. Pfaller, D. J. Diekema *et al.*, 2009 Initial treatment and outcome of Candida glabrata *vs.* Candida albicans bloodstream infection. Diagn. Microbiol.

Infect. Dis. 64: 152–157. https://doi.org/10.1016/j.diagmicrobio.2009.03.007

Kueng, S., M. Oppikofer, and S. M. Gasser, 2013 SIR proteins and the assembly of silent chromatin in budding yeast. Annu. Rev. Genet. 47: 275–306. https://doi.org/10.1146/annurev-genet-021313-173730

Kyrion, G., K. Liu, C. Liu, and A. J. Lustig, 1993 RAP1 and telomere structure regulate telomere position effects in Saccharomyces cerevisiae. Genes Dev. 7: 1146–1159. https://doi.org/10.1101/gad.7.7a.1146

Lebrun, E., E. Revardel, R. Li, and E. Gilson, 2001 Protosilencers in Saccharomyces cerevisiae subtelomeric regions. Genetics 158: 167–176.

Levis, R. W., R. Ganesan, K. Houtchens, L. A. Tolar, and F. M. Sheen, 1993 Transposons in place of telomeric repeats at a Drosophila telomere. Cell 75: 1083–1093. https://doi.org/10.1016/0092-8674(93)90318-K

Liu, Z., and W. T. Garrard, 2005 Long-range interactions between three transcriptional enhancers, active Vkappa gene promoters, and a 3' boundary sequence spanning 46 kilobases. Mol. Cell. Biol. 25: 3220–3231. https://doi.org/10.1128/MCB.25.8.3220-3231.2005

Luo, K., M. A. Vega-Palas, and M. Grunstein, 2002 Rap1-Sir4 binding independent of other Sir, yKu, or histone interactions initiates the assembly of telomeric heterochromatin in yeast. Genes Dev. 16: 1528–1539. https://doi.org/10.1101/gad.988802

Mathelier, A., O. Fornes, D. J. Arenillas, C. Y. Chen, G. Denay *et al.*, 2016 JASPAR 2016: a major expansion and update of the open-access database of transcription factor binding profiles. Nucleic Acids Res. 44: D110–D115. https://doi.org/10.1093/nar/gkv1176

Miele, A., K. Bystricky, and J. Dekker, 2009 Yeast silent mating type loci form heterochromatic clusters through silencer protein-dependent long-range interactions. PLoS Genet. 5: e1000478. https://doi.org/10.1371/journal.pgen.1000478

Moretti, P., and D. Shore, 2001 Multiple interactions in sir protein recruitment by Rap1p at silencers and telomeres in yeast. Mol. Cell. Biol. 21: 8082–8094. https://doi.org/10.1128/MCB.21.23.8082-8094.2001

Moretti, P., K. Freeman, L. Coodly, and D. Shore, 1994 Evidence that a complex of SIR proteins interacts with the silencer and telomere-binding protein RAP1. Genes Dev. 8: 2257–2269. https://doi.org/10.1101/gad.8.19.2257

Nimmo, E. R., G. Cranston, and R. C. Allshire, 1994 Telomere-associated chromosome breakage in fission yeast results in variegated expression of adjacent genes. EMBO J. 13: 3801–3811.

Orta-Zavalza, E., G. Guerrero-Serrano, G. Gutiérrez-Escobedo, I. Cañas-Villamar, J. Juárez-Cepeda *et al.*, 2013 Local silencing controls the oxidative stress response and the multidrug resistance in Candida glabrata. Mol. Microbiol. 88: 1135–1148. https://doi.org/10.1111/mmi.12247

Palladino, F., T. Laroche, E. Gilson, A. Axelrod, L. Pillus *et al.*, 1993 SIR3 and SIR4 proteins are required for the positioning and integrity of yeast telomeres. Cell 75: 543–555. https://doi.org/10.1016/0092-8674(93)90388-7

Pfaller, M. A., and D. J. Diekema, 2007 Epidemiology of invasive candidiasis: a persistent public health problem. Clin. Microbiol. Rev. 20: 133–163. https://doi.org/10.1128/CMR.00029-06

Pryde, F. E., and E. J. Louis, 1999 Limitations of silencing at native yeast telomeres. EMBO J. 18: 2538–2550. https://doi.org/10.1093/emboj/18.9.2538

Robledo-Márquez, K., G. Gutiérrez-Escobedo, P. Yáñez-Carrillo, Y. Vidal-Aguiar, M. Briones-Martín-del-Campo *et al.*, 2016 Candida glabrata encodes a longer variant of the mating type (MAT) alpha2 gene in the mating type-like MTL3 locus, which can form homodimers. FEMS Yeast Res. 16: fow082. https://doi.org/10.1093/femsyr/fow082

Rosas-Hernández, L. L., A. Juárez-Reyes, O. E. Arroyo-Helguera, A. De Las Peñas, S.-J. Pan *et al.*, 2008 yKu70/yKu80 and Rif1 regulate silencing differentially at telomeres in Candida glabrata. Eukaryot. Cell 7: 2168–2178. https://doi.org/10.1128/EC.00228-08

Scherf, A., R. Hernandez-Rivas, P. Buffet, E. Bottius, C. Benatar *et al.*, 1998 Antigenic variation in malaria: in situ switching, relaxed and mutually exclusive transcription of var genes during intra-erythrocytic development in Plasmodium falciparum. EMBO J. 17: 5418–5426. https://doi.org/10.1093/emboj/17.18.5418

Therizols, P., T. Duong, B. Dujon, C. Zimmer, and E. Fabre, 2010 Chromosome arm length and nuclear constraints determine the dynamic relationship of yeast subtelomeres. Proc. Natl. Acad. Sci. USA 107: 2025–2030. https://doi.org/10.1073/pnas.0914187107

Thurtle, D. M., and J. Rine, 2014 The molecular topography of silenced chromatin in Saccharomyces cerevisiae. Genes Dev. 28: 245–258. https://doi.org/10.1101/gad.230532.113

Valenzuela, L., N. Dhillon, R. N. Dubey, M. R. Gartenberg, and R. T. Kamakaka, 2008 Long-range communication between the silencers of HMR. Mol. Cell. Biol. 28: 1924–1935. https://doi.org/10.1128/MCB.01647-07

Communicating editor: M. Freitag